Backscattering in helical edge states from a magnetic impurity and Rashba disorder

Lukas Kimme,[1] Bernd Rosenow,[1] and Arne Brataas[2]

[1]*Institut für Theoretische Physik, Universität Leipzig, D-04103 Leipzig, Germany*
[2]*Department of Physics, Norwegian University of Science and Technology, NO-7491 Trondheim, Norway*

Transport by helical edge states of a quantum spin Hall insulator is experimentally characterized by a weakly temperature-dependent mean free path of a few microns and by reproducible conductance oscillations, challenging proposed theoretical explanations. We consider a model where edge electrons experience spatially random Rashba spin-orbit coupling and couple to a magnetic impurity with spin $S \geqslant 1/2$. In a finite bias steady state, we find for $S > 1/2$ an impurity induced resistance with a temperature dependence in agreement with experiments. Since backscattering is elastic, interference between different scatterers possibly explains conductance fluctuations.

Introduction. During the last decade, the quantum spin Hall effect (QSHE) [1–3] has become an important example of a topologically ordered state with time-reversal invariance. One of its key features is the existence of helical edge states [4] with a quantized conductance of e^2/h per edge, as edge electrons are protected from elastic single particle backscattering by time-reversal symmetry [1,4,5]. Soon after the theoretical prediction [6], the QSHE was realized in HgTe/CdTe quantum wells [7], and the quantized conductance [7] as well as the demonstration of nonlocal transport [8] were crucial signatures for this first-time experimental observation. However, already in this first as well as in subsequent experiments [7–12], deviations from the quantized conductance with a weak temperature dependence were found for edges longer than approximately 1 μm. Moreover, in short samples, where the conductance is essentially quantized, small conductance fluctuations are observed as the back-gate voltage is tuned [7,8,12,13]. After the prediction [14] of the QSHE in InAs/GaSb/AlSb quantum wells, the same qualitative behavior of the conductance as in HgTe/CdTe was observed also in these devices [15–18].

A multitude of other mechanisms beyond elastic single particle backscattering have been proposed as possible explanations for the relatively short mean free path [19]: inelastic single particle [20–23] and two-particle backscattering [1,4,5,23–25] which can be caused by electron-electron or electron-phonon interactions, both of which are usually considered in combination with other time-reversal invariant perturbations; tunneling of electrons into charge puddles caused by inhomogeneous doping, giving rise to inelastic single particle backscattering [26,27]; coupling of edge electrons to a spin bath which gets dynamically polarized [28], thus effectively breaking time-reversal symmetry and giving rise to elastic backscattering in conjunction with Rashba disorder [29]; time-reversal symmetry breaking by an exciton condensate [30]; and coupling of edge electrons to a single Kondo impurity [4,31,32], to a lattice of Kondo impurities [33], to a single Kondo impurity in the presence of homogeneous Rashba spin-orbit coupling [34,35], or to several Kondo impurities with random anisotropies [36]. Although these mechanisms are very diverse, many of them have in common a pronounced temperature dependence, usually some power law T^α with positive exponent α for the resistance. However, only a weak temperature dependence has been observed

experimentally, with the exception of a recent study using very low excitation currents [37]. In fact, in some experiments, a slight increase of the resistance is observed when the temperature is decreased [7,11,12]. With respect to the conductance fluctuations, only charge puddles [26,27] as well as coherent scattering between several magnetic impurities with large spin $S > 1$ and uniaxial single-ion anisotropy [38] were considered as possible explanations. Theories that build on scattering from local disorder are also supported by recent scanning gate microscopy experiments [39], which identified individual scattering centers.

In this Rapid Communication, we consider scattering of helical edge electrons from a magnetic impurity with spin $S \geqslant 1/2$ in combination with a spatially fluctuating Rashba spin-orbit coupling. The latter originates from a fluctuating electric field in the out-of-plane direction due to disorder in the doping layers [40–44]. From a T-matrix calculation accounting for the combined scattering events off these perturbations, we derive an effective additional coupling to the impurity. This coupling provides a backscattering mechanism which is enhanced by an increased polarization of the impurity with spin $S > 1/2$. The polarization of the impurity spin is determined from the steady state solution to a semiclassical scattering rate equation. We consider the linear and the nonlinear regime. Upon entering the nonlinear regime with the source drain voltage larger than temperature, the impurity gets polarized and the Rashba disorder induced effective coupling leads to an increased resistance, thus providing a possible explanation for the experimental results. We assume that the relevant Kondo temperature is exponentially suppressed and well below the temperature regime studied in our analysis. Since the dominant contribution to backscattering is elastic in our model, quantum interference between different scatterers is possible, and can give rise to conductance fluctuations as observed in Refs. [7,8,12,13].

Model. The edge states are described by

$$H_0 = \int dx\, \Psi^\dagger_\alpha(x)\sigma^z_{\alpha\beta}(-i v\hbar\partial_x)\Psi_\beta(x), \qquad (1)$$

where $\Psi_\uparrow(x)$ annihilates a right-moving electron, v is the edge velocity, and the spin quantization axis is in the z direction. A
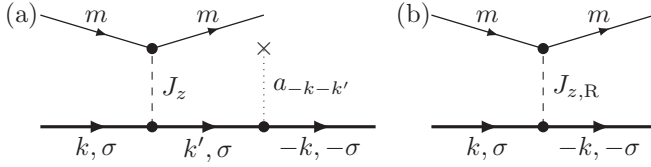
FIG. 1. (a) Diagrammatic representation of the second-order scattering process that gives rise to elastic backscattering without an impurity spin flip [cf. Eq. (4)]. (b) The corresponding first-order process from the effective coupling H'_S [cf. Eq. (5)]. The dashed line denotes the (effective) coupling of the impurity and electron. The dotted line with a cross represents the Rashba potential.

disordered Rashba spin-orbit coupling is described by [40–43]

$$H_R = \int dx \, \Psi^\dagger_\alpha(x) \sigma^y_{\alpha\beta} \{a(x), i\partial_x\} \Psi_\beta(x), \tag{2}$$

with the correlator $\langle a(x)a(x')\rangle_{\mathrm{dis}} = V_0 F(x - x')$ and $F(0) = 1$ [44,45]. Being time-reversal invariant, H_R does not cause elastic backscattering [1]. The essential ingredient is the coupling of electrons to a local magnetic impurity with spin S via

$$H_S = J_z S^z s^z + J_\perp(S^+ s^- + S^- s^+) + J_{\mathrm{aniso}}(S^+ + S^-)s^z. \tag{3}$$

As usual, $S^\pm = S^x \pm i S^y$ and $s^i = \Psi^\dagger_\alpha(0)\sigma^i_{\alpha\beta}\Psi_\beta(0)$ are the local spin density operators of the edge electrons. For $J_{\mathrm{aniso}} = 0$, H_S describes a Heisenberg XXZ coupling, which has an axial rotation symmetry and was the subject of earlier studies [4,31–35]. In systems with axial symmetric H_S, the z component of the total spin is conserved and the dc conductance is exactly quantized [32]. A finite J_{aniso} breaks the axial rotation symmetry, thus enabling persistent backscattering in the dc limit [46].

In general, a coupling to the impurity spin could also involve terms such as $S^+ s^+ + S^- s^-$ and $S^z(s^+ + s^-)$ that break axial rotation symmetry. However, a microscopic analysis, based on an isotropic sp-d exchange interaction of bulk electrons with the impurity, results only in the terms in Eq. (3), at least for HgTe/CdTe quantum wells [45]. Nevertheless, as we will explain, the combined processes of impurity and Rashba disorder scattering effectively give rise to such additional terms.

Effective couplings from second-order processes. We now consider the combined scattering from the impurity and the Rashba disorder by using the T matrix $T(\epsilon) = (H_S + H_R) + (H_S + H_R)G(\epsilon)T$, with $G(\epsilon) = (\epsilon - H_0)^{-1}$. The T-matrix element associated with the first term of Eqs. (3) and (2) is

$$\langle m; -k, -\sigma | T_{z,R}(\epsilon_i) | m; k, \sigma \rangle$$
$$= \frac{\sigma i J_z \langle m|S^z|m\rangle}{L\sqrt{L}} \sum_{k'} \left(\frac{(k-k')a_{-k-k'}}{\hbar v(k-k')} + \frac{(k'+k)a_{k'-k}}{\hbar v(k'+k)} \right) \tag{4}$$

(cf. Fig. 1). Here, $|m; k, \sigma\rangle$ denotes a product state of the local moment in the S^z eigenstate $|m\rangle$ and an electron with helical spin σ and momentum $\hbar k$, L the distance between the left and right reservoir, $\epsilon_i = \sigma v \hbar k$ the energy of the initial state $|m; k, \sigma\rangle$, and a_q the Fourier components of $a(x)$. The energy

difference between the initial and intermediate state in the denominator compensates the matrix element from Rashba disorder in the numerator.

With regard to scattering rates, to be discussed below, the second-order process described in Eq. (4) can effectively be described as a first-order process resulting from the additional anisotropic coupling

$$H'_S = J_{z,R} S^z(s^+ + s^-). \tag{5}$$

Here, $J_{z,R} = 2\sqrt{\eta} J_z$ is an effective coupling constant with $\eta = V_0/\hbar^2 v^2$. Analogously to the combined process described by $T_{z,R}$, there are also second-order processes where electrons scatter from the Rashba disorder and from the impurity by either the $J_\perp$ or the J_{aniso} term of H_S in Eq. (3). Again, these effects can be captured by considering first-order processes from the effective couplings $J_{\perp,R}(S^+ + S^-)s^z$ and $J_{\mathrm{aniso},R}(S^+s^+ + S^+s^- + \mathrm{H.c.})$, with $J_{\perp,R} = \sqrt{\eta} J_\perp$ and $J_{\mathrm{aniso},R} = 2\sqrt{\eta} J_{\mathrm{aniso}}$, respectively. $J_{\perp,R}$ only renormalizes the J_{aniso} coupling already present in H_S. In contrast, $J_{\mathrm{aniso},R}$, besides renormalizing $J_\perp$, opens an additional scattering channel via the $S^+s^+ + S^-s^-$ terms.

Scattering rates. Since we are interested in the effect of the impurity on dc transport, we pursue two aims: (i) We want to achieve a description of the impurity spin in a driven steady state, and (ii) we want to compute the transport scattering rates determining the impurity induced dc resistance. To achieve (i), we calculate the integrated rates $\Gamma^{\sigma'\sigma}_{m'm}$, which characterize the scattering of an electron from an initial state with helical spin σ into a final state with helical spin σ', as the impurity spin is flipped from $|m\rangle$ to $|m'\rangle$. $\Gamma^{\sigma'\sigma}_{m'm}$ are obtained by weighting the rates for scattering from $|m; k, \sigma\rangle$ to $|m'; k', \sigma'\rangle$ with the probability for the initial and final state to be occupied or unoccupied, respectively, and then summing over initial and final momenta. To calculate the individual rates, we employ Fermi's golden rule for H^{eff}_S, including all original and effective impurity couplings. For temperatures and voltages much smaller than the bulk excitation gap of the topological insulator, the weak momentum dependence of $\langle m'; k', \sigma' | H^{\mathrm{eff}}_S | m; k, \sigma \rangle$ can be neglected. For forward scattering with $\sigma' = \sigma$, we then find

$$\Gamma^{\sigma\sigma}_{m'm}(\beta) = \frac{L^2}{2\pi \hbar^3 v^2 \beta} |\langle m'; \sigma | H^{\mathrm{eff}}_S | m; \sigma \rangle|^2, \tag{6}$$

where the temperature dependence is due to the integrated occupation factors $\int dE \, f_\sigma(1 - f_\sigma) = 1/\beta$. Here, $f_\uparrow$ ($f_\downarrow$) denotes the Fermi distribution function describing the occupation of right-moving (left-moving) electrons from the left (right) reservoir. In the case of backscattering $\sigma' = -\sigma$, the rates involve occupation factors $f_\sigma(1 - f_{-\sigma})$, leading to a voltage dependence

$$\Gamma^{-\sigma\sigma}_{m'm}(\beta, eV) = \frac{L^2}{2\pi \hbar^3 v^2 \beta} |\langle m'; -\sigma | H^{\mathrm{eff}}_S | m; \sigma \rangle|^2 I^\sigma(\beta eV), \tag{7}$$

where

$$I^\sigma \equiv \beta \int dE \, f_\sigma(1 - f_{-\sigma}) = \sigma \beta eV \frac{e^{\sigma \beta eV}}{e^{\sigma \beta eV} - 1}. \tag{8}$$

At low bias voltage, $\beta eV \ll 1$, $I^\sigma \simeq 1$ so that the forward and backscattering rates have the same temperature dependence.

TABLE I. Results for the integrated scattering rates $\Gamma_{mm'}^{\sigma\sigma'}$.

Process	$\Gamma \times (2\pi\hbar^3 v^2 \beta/L^2)$
$\|m;\sigma\rangle \rightarrow \|m;-\sigma\rangle$	$J_{z,\mathrm{R}}^2\|\langle m\|S^z\|m\rangle\|^2 I^\sigma$
$\|m;\uparrow\rangle \rightarrow \|m+1;\downarrow\rangle$	$(J_\perp^2 + J_{\mathrm{aniso,R}}^2)\|\langle m+1\|S^+\|m\rangle\|^2 I^\uparrow$
$\|m;\uparrow\rangle \rightarrow \|m-1;\downarrow\rangle$	$J_{\mathrm{aniso,R}}^2\|\langle m-1\|S^-\|m\rangle\|^2 I^\uparrow$
$\|m;\sigma\rangle \rightarrow \|m\pm 1;\sigma\rangle$	$(J_{\mathrm{aniso}}^2 + J_{\perp,\mathrm{R}}^2)\|\langle m\pm 1\|S^\pm\|m\rangle\|^2$

On the other hand, when $\beta eV \gg 1$, the backscattering of right movers is linearly enhanced, while the backscattering of left movers is exponentially suppressed. For detailed results, see Table I.

Master equation. We describe the state of the impurity by a density matrix ρ and assume that dephasing from the coupling to the electron bath is sufficiently strong, such that we can neglect coherences and consider $\rho = \sum_m P_m |m\rangle\langle m|$ to be diagonal in the basis of eigenstates of S^z, $S^z|m\rangle = m|m\rangle$. We can then proceed to determine the steady state of the impurity spin at finite temperature and under an applied transport voltage V from the master equation

$$\partial_t P_m = \sum_{m'} (\Gamma_{mm'} P_{m'} - \Gamma_{m'm} P_m), \qquad (9)$$

where $\Gamma_{m'm} = \sum_{\sigma'\sigma} \Gamma_{m'm}^{\sigma'\sigma}$. In a steady state, $\partial_t P_m = 0$, and we find the recursively defined solution $P_{m-1} = \zeta P_m$, with $\zeta = \Gamma_{m-1,m}/\Gamma_{m,m-1}$. ζ depends on βeV and the (effective) coupling constants, but not on m because the m-dependent matrix elements of the ladder operators $S^\pm$ cancel. We provide an explicit expression in the Supplemental Material [45]. For the model considered here, we have $0 \leqslant \zeta \leqslant 1$ and the two limiting cases have simple solutions: $\zeta = 0$ implies $P_m = \delta_{m,S}$ and corresponds to a maximally polarized local moment, while for $\zeta = 1$ the impurity is completely unpolarized, i.e., $P_m = 1/(2S+1)$. Notice that $\beta eV = 0$ implies $\zeta = 1$, because, without an applied transport voltage, there is no asymmetry between the rates for forward and backscattering [cf. Eqs. (6) and (7)]. The general dependence of P_m on m interpolates between the two limiting cases:

$$P_m = \frac{(1-\zeta)\zeta^S}{1-\zeta^{1+2S}}\left(\frac{1}{\zeta}\right)^m. \qquad (10)$$

Impurity induced resistance. The backscattering probability R can be related to a scattering rate $1/\tau$ by multiplying with the time of flight L/v. This compensates a dependence $1/\tau \propto 1/L$ in all scattering rates, due to the normalization of the plane wave with a factor $1/\sqrt{L}$. In this way, both R and the edge conductance $G = (1-R)e^2/h$ are independent of the system size L, as expected for a single scattering site. For $R \ll 1$, R equals the impurity induced resistance normalized by h/e^2. From the effective impurity coupling we have two important backscattering mechanisms [48], and hence obtain

$$R = \frac{L}{v}\left(\frac{1}{\tau_{z,\mathrm{R}}} + \frac{1}{\tau_\perp}\right), \qquad (11)$$

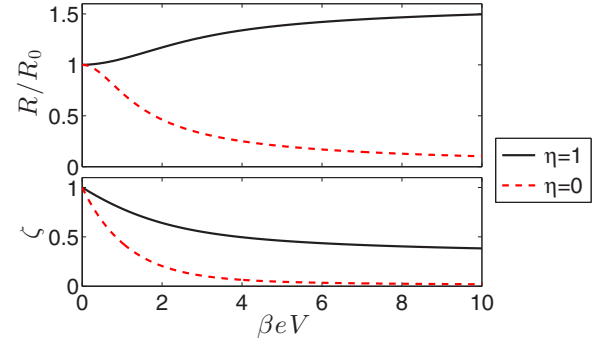where a Fermi's golden rule calculation yields

FIG. 2. The normalized impurity induced backscattering probability R/R_0 and ζ, both in dependence of the ratio of transport voltage and temperature βeV. R_0 is the backscattering probability for $\beta eV \ll 1$. In both cases, $S = 5/2$ and $J_z^2/J_\perp^2 = J_\perp^2/J_{\mathrm{aniso}}^2 = 10$. R_0 is enhanced by two orders of magnitude as the dimensionless strength of Rashba disorder η is increased from 0 to 1.

$$\frac{1}{\tau_\perp} = \frac{J_\perp^2 + J_{\mathrm{aniso,R}}^2}{\hbar^2 vL} p_\perp \sum_{m=-S}^{S-1} |\langle m+1|S^+|m\rangle|^2 P_m, \qquad (12a)$$

$$\frac{1}{\tau_{z,\mathrm{R}}} = \frac{J_{z,\mathrm{R}}^2}{\hbar^2 vL} \sum_{m=-S}^{S} |\langle m|S^z|m\rangle|^2 P_m. \qquad (12b)$$

Here, $p_\perp = 1 - \Gamma_{m,m+1}^{\uparrow\downarrow}/\Gamma_{m,m+1}$ accounts for the fact that the dc resistance is affected only by those backscattering events of right-moving electrons which are *not* compensated by a subsequent backscattering of a left-moving electron [45]. For example, in the case of vanishing Rashba disorder and H_S with axial rotation symmetry, we find $\Gamma_{m,m+1}^{\uparrow\downarrow} = \Gamma_{m,m+1}$, hence $p_\perp$ vanishes.

Results. Although the framework that we set up so far does not rely on any specific assumptions about the couplings in H_S, it is helpful to focus on the parameter regime $J_z^2 \gg J_\perp^2 \gg J_{\mathrm{aniso}}^2$ for three reasons: (i) From a microscopic analysis we found that this regime is experimentally relevant for HgTe/CdTe quantum wells [45]. (ii) The importance of the Rashba disorder induced effective couplings with regard to the dc resistance becomes particularly clear in this parameter regime. (iii) A clear hierarchy of couplings allows one to disentangle the discussion of scattering processes. The following detailed discussion about the relevancy of Rashba disorder for the impurity induced resistance leads to two important results: First, while $R(\beta eV)$ is a monotonically decreasing function without Rashba disorder, this monotonicity is reversed in the presence of Rashba disorder (see Fig. 2). Second, R_0, the backscattering probability in the limit $\beta eV \ll 1$, is significantly increased by Rashba disorder.

Let us consider first the case where Rashba disorder is absent, i.e., $\eta = 0$. The only nonvanishing backscattering rate is $1/\tau_\perp$ from Eq. (12a), which is small as it arises from an interplay of scattering due to $J_\perp$ and J_{aniso}. In particular, R_0 is found to be proportional to the harmonic mean of $J_\perp^2$ and $2J_{\mathrm{aniso}}^2$, because $p_\perp = [1 + J_\perp^2/2J_{\mathrm{aniso}}^2]^{-1}$ for $\beta eV = 0$. Consequently, when $J_\perp^2$ and J_{aniso}^2 are very different in magnitude, it is the smaller of the two which determines
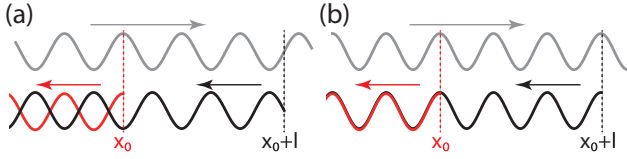
FIG. 3. A right-moving wave (gray) is phase coherently backscattered from impurities at x_0 (red) and $x_0 + l$ (black). Destructive (constructive) interference occurs when $k_F l = \nu\pi$ with half-integer (integer) ν—cf. (a) [(b)].

the magnitude of R_0. With increasing βeV, the backscattering of right movers via $J_\perp S^+ s^-$ becomes increasingly dominant relative to other scattering rates and tends to polarize the impurity, such that $\zeta \simeq 2 J_{\mathrm{aniso}}^2/\beta eV J_\perp^2$ approaches zero in the large βeV limit (cf. Fig. 2). With increasing polarization, the probability for the impurity spin to be in state $|S\rangle$ increases, and the probability for an individual right-moving electron to be backscattered is suppressed. This leads to the monotonic decrease of $R(\beta eV)$ shown in Fig. 2, with $R \sim J_{\mathrm{aniso}}^2/\beta eV$ in the large βeV limit [49].

Rashba disorder, described by a finite η, has a profound effect on the impurity induced resistance. Since $J_z^2 \gg J_\perp^2 \gg J_{\mathrm{aniso}}^2$, $1/\tau_{z,\mathrm{R}}$ dominates $1/\tau_\perp$ already for very weak Rashba disorder with $\eta \gtrsim 4 J_{\mathrm{aniso}}^2/J_z^2$. The magnitude of R_0 is then determined by $J_{z,\mathrm{R}}^2$ instead of J_{aniso}^2, which, depending on the precise values of the couplings and η, can be a large difference. Regarding the dependence on the polarization, $1/\tau_{z,\mathrm{R}}$ is qualitatively different from $1/\tau_\perp$. Evaluating the sum over m in Eq. (12b) for the limiting cases of perfect polarization, $P_m = \delta_{m,S}$, and vanishing polarization, $P_m = 1/(2S+1)$, yields S^2 in the former and $S(S+1)/3$ in the latter case, respectively. This shows that, for spin $S > 1/2$, the rate $1/\tau_{z,\mathrm{R}}$ increases with increasing polarization, because

$S^2 > S(S+1)/3$. However, $1/\tau_{z,\mathrm{R}}$ is independent of ζ for $S = 1/2$. Thus, in contrast to the case without Rashba disorder, R is now found to monotonically increase with βeV when $S > 1/2$.

For real samples with several impurities, the total backscattering rate is proportional to the number of impurities in the absence of localization. Based on Eq. (11), we estimate the mean free path to be 4 μm in 7.0 nm wide HgTe quantum wells with a lattice constant $a = 0.65$ nm and $v = 4 \times 10^5$ m/s, by assuming (i) that there is a concentration of 10^{-4} Mn^{2+} ions ($S = 5/2$) per unit cell, (ii) $\zeta = 0.5$ and spatial average $\langle J_z^2/\hbar^2 v^2 \rangle = 0.035$ [45], and (iii) $\eta \approx 3$ based on the estimate for V_0 from Refs. [29,44].

A plane wave $e^{ik_F x}$ with Fermi momentum k_F can be backscattered elastically from impurities at x_0 and $x_0 + l$ by the process Eq. (4) (see Fig. 3). The partial waves $e^{-ik_F(x-x_0)+ik_F x_0}$ and $e^{-ik_F(x-x_0-l)+ik_F(x_0+l)}$ interfere, resulting in a contribution to the backscattering probability $\propto \cos k_F l$. Tuning k_F via a back-gate voltage alternately causes constructive or destructive interference. Hence, conductance fluctuations occur, in agreement with experiment. Several impurities give rise to more complex oscillations.

Summary. We determined the dc resistance of helical edge states in the presence of Rashba disorder and a magnetic impurity with spin $S > 1/2$. As a key result, we find that combined scattering from both Rashba disorder and impurity is enhanced as the impurity becomes more polarized, giving rise to a resistance that slowly increases as the ratio of transport voltage and temperature increases, in agreement with experiments [7,11,12]. Since backscattering is elastic, quantum interference can explain the occurrence of conductance fluctuations.

[1] C. L. Kane and E. J. Mele, Phys. Rev. Lett. **95**, 226801 (2005).

[2] C. L. Kane and E. J. Mele, Phys. Rev. Lett. **95**, 146802 (2005).

[3] B. A. Bernevig and S.-C. Zhang, Phys. Rev. Lett. **96**, 106802 (2006).

[4] C. Wu, B. A. Bernevig, and S.-C. Zhang, Phys. Rev. Lett. **96**, 106401 (2006).

[5] C. Xu and J. E. Moore, Phys. Rev. B **73**, 045322 (2006).

[6] B. A. Bernevig, T. L. Hughes, and S.-C. Zhang, Science **314**, 1757 (2006).

[7] M. König, S. Wiedmann, C. Brüne, A. Roth, H. Buhmann, L. W. Molenkamp, X.-L. Qi, and S.-C. Zhang, Science **318**, 766 (2007).

[8] A. Roth, C. Brüne, H. Buhmann, L. W. Molenkamp, J. Maciejko, X.-L. Qi, and S.-C. Zhang, Science **325**, 294 (2009).

[9] K. C. Nowack, E. M. Spanton, M. Baenninger, M. König, J. R. Kirtley, B. Kalisky, C. Ames, P. Leubner, C. Brüne, H. Buhmann, L. W. Molenkamp, D. Goldhaber-Gordon, and K. A. Moler, Nat. Mater. **12**, 787 (2013).

[10] G. Grabecki, J. Wróbel, M. Czapkiewicz, Ł. Cywiński, S. Gierałtowska, E. Guziewicz, M. Zholudev, V. Gavrilenko, N. N. Mikhailov, S. A. Dvoretski, F. Teppe, W. Knap, and T. Dietl, Phys. Rev. B **88**, 165309 (2013).

[11] G. M. Gusev, Z. D. Kvon, E. B. Olshanetsky, A. D. Levin, Y. Krupko, J. C. Portal, N. N. Mikhailov, and S. A. Dvoretsky, Phys. Rev. B **89**, 125305 (2014).

[12] A. Yacoby (private communication).

[13] M. König, H. Buhmann, L. W. Molenkamp, T. Hughes, C.-X. Liu, X.-L. Qi, and S.-C. Zhang, J. Phys. Soc. Jpn. **77**, 031007 (2008).

[14] C. Liu, T. L. Hughes, X.-L. Qi, K. Wang, and S.-C. Zhang, Phys. Rev. Lett. **100**, 236601 (2008).

[15] I. Knez, R.-R. Du, and G. Sullivan, Phys. Rev. Lett. **107**, 136603 (2011).

[16] K. Suzuki, Y. Harada, K. Onomitsu, and K. Muraki, Phys. Rev. B **87**, 235311 (2013).

[17] I. Knez, C. T. Rettner, S.-H. Yang, S. S. P. Parkin, L. Du, R.-R. Du, and G. Sullivan, Phys. Rev. Lett. **112**, 026602 (2014).

[18] E. M. Spanton, K. C. Nowack, L. Du, G. Sullivan, R.-R. Du, and K. A. Moler, Phys. Rev. Lett. **113**, 026804 (2014).

[19] G. Dolcetto, M. Sassetti, and T. L. Schmidt, arXiv:1511.06141.

[20] T. L. Schmidt, S. Rachel, F. von Oppen, and L. I. Glazman, Phys. Rev. Lett. **108**, 156402 (2012).

[21] J. C. Budich, F. Dolcini, P. Recher, and B. Trauzettel, Phys. Rev. Lett. **108**, 086602 (2012).

[22] N. Lezmy, Y. Oreg, and M. Berkooz, Phys. Rev. B **85**, 235304 (2012).

[23] N. Kainaris, I. V. Gornyi, S. T. Carr, and A. D. Mirlin, Phys. Rev. B **90**, 075118 (2014).

[24] F. Crépin, J. C. Budich, F. Dolcini, P. Recher, and B. Trauzettel, Phys. Rev. B **86**, 121106 (2012).

[25] F. Geissler, F. Crépin, and B. Trauzettel, Phys. Rev. B **89**, 235136 (2014).

[26] J. I. Väyrynen, M. Goldstein, and L. I. Glazman, Phys. Rev. Lett. **110**, 216402 (2013).

[27] J. I. Väyrynen, M. Goldstein, Y. Gefen, and L. I. Glazman, Phys. Rev. B **90**, 115309 (2014).

[28] A. M. Lunde and G. Platero, Phys. Rev. B **86**, 035112 (2012).

[29] A. Del Maestro, T. Hyart, and B. Rosenow, Phys. Rev. B **87**, 165440 (2013).

[30] D. I. Pikulin and T. Hyart, Phys. Rev. Lett. **112**, 176403 (2014).

[31] J. Maciejko, C. Liu, Y. Oreg, X.-L. Qi, C. Wu, and S.-C. Zhang, Phys. Rev Lett. **102**, 256803 (2009).

[32] Y. Tanaka, A. Furusaki, and K. A. Matveev, Phys. Rev. Lett. **106**, 236402 (2011).

[33] J. Maciejko, Phys. Rev. B **85**, 245108 (2012).

[34] E. Eriksson, A. Ström, G. Sharma, and H. Johannesson, Phys. Rev. B **86**, 161103 (2012); **87**, 079902(E) (2013).

[35] E. Eriksson, Phys. Rev. B **87**, 235414 (2013).

[36] B. L. Altshuler, I. L. Aleiner, and V. I. Yudson, Phys. Rev. Lett. **111**, 086401 (2013).

[37] T. Li, P. Wang, H. Fu, L. Du, K. A. Schreiber, X. Mu, X. Liu, G. Sullivan, G. A. Csthy, X. Lin, and R.-R. Du, Phys. Rev. Lett. **115**, 136804 (2015).

[38] V. Cheianov and L. I. Glazman, Phys. Rev. Lett. **110**, 206803 (2013).

[39] M. König, M. Baenninger, A. G. F. Garcia, N. Harjee, B. L. Pruitt, C. Ames, P. Leubner, C. Brüne, H. Buhmann, L. W. Molenkamp, and D. Goldhaber-Gordon, Phys. Rev. X **3**, 021003 (2013).

[40] E. Y. Sherman, Phys. Rev. B **67**, 161303 (2003).

[41] L. E. Golub and E. L. Ivchenko, Phys. Rev. B **69**, 115333 (2004).

[42] A. Ström, H. Johannesson, and G. I. Japaridze, Phys. Rev. Lett. **104**, 256804 (2010).

[43] D. G. Rothe, R. W. Reinthaler, C.-X. Liu, L. W. Molenkamp, S.-C. Zhang, and E. M. Hankiewicz, New J. Phys. **12**, 065012 (2010).

[44] M. M. Glazov, E. Y. Sherman, and V. K. Dugaev, Physica E **42**, 2157 (2010).

[45] See Supplemental Material at http://link.aps.org/supplemental/10.1103/PhysRevB.93.081301 for a derivation of H_S, details about the effective couplings, and explicit expressions for ζ and $p_\perp$.

[46] A coupling analogous to J_{aniso} has been discussed in the context of hyperfine interactions [47].

[47] A. M. Lunde and G. Platero, Phys. Rev. B **88**, 115411 (2013).

[48] In Eq. (11), we omit a third scattering rate arising from the effective coupling $J_{\mathrm{aniso,R}}(S^+ s^+ + S^- s^-)$, because its impact on the backscattering probability is negligible in all situations that we are interested in.

[49] We suppressed in our discussion the fact that $p_\perp$ increases with βeV and approaches 1 for $\beta eV \gg 1$. However, a detailed analysis shows that $R(\beta eV)$ does not have a local maximum, i.e., effects due to varying polarization dominate.